IEEE Access
Multidisciplinary | Rapid Review | Open Access Journal

Date of publication xxxx 00, 0000, date of current version xxxx 00, 0000.

Digital Object Identifier 10.1109/ACCESS.2021.Doi Number

LMSRE-Based Adaptive PI Controller for Enhancing the Performance of an Autonomous Operation of Microgrids

Ahmed M. Hussien[1], Rania A. Turky[1], Hany M. Hasanien[2], Senior Member, IEEE, and Ahmed Al-Durra[3], Senior Member, IEEE

[1]Electrical Engineering Department, Faculty of Engineering and Technology, Future University in Egypt, Cairo, Egypt, 11835. (e-mails: ahmed.moreab@fue.edu.eg, Rania.turky@fue.edu.eg)

[2]Electrical Power and Machines Department, Faculty of Engineering, Ain Shams University, Cairo 11517, Egypt. (e-mails: hanyhasanien@ieee.org)

[3]Advanced Power and Energy Center, Department of Electrical Engineering and Computer Science, Khalifa University, Abu Dhabi 127788, United Arab Emirates. (e-mail: ahmed.aldurra@ku.ac.ae)

Corresponding author: Ahmed Al-Durra (ahmed.aldurra@ku.ac.ae)

ABSTRACT Microgrids take a large part in power networks thanks to their operational and economic benefits. This research introduces a novel implementation of an adaptive proportional plus integral (PI) controller to boost the autonomous microgrid operation efficiency. The least mean and square roots of the exponential algorithm are utilized in the adaptive PI control strategy. The multi-objective function for both sunflower optimization (SFO) and particle swarm optimization (PSO) algorithms is obtained by The Response Surface Methodology. The system is evaluated under different environments, which are stated as follows: 1) disconnect the system from the grid (islanding), 2) autonomous system exposure to load variability, and 3) autonomous system exposure to a symmetrical fault. The proposed practicality of the control plan is shown by the data of the simulation, which is extracted from PSCAD/EMTDC software. The strength of the suggested adaptive control is confirmed through matching its results with those obtained using the SFO and PSO based optimal PI controllers.

INDEX TERMS microgrid; optimization; power systems; renewable energy.

I. INTRODUCTION

A. Literature review

The large centralized generation stations continue struggling to satisfy the growth in demand. That's why the trend in generation nowadays is looking towards the smaller distributed generation (DG) networks, situated near to the load centers. This minimizes the transmission losses and stops the rapid expansion of the transmission network. The value of the DG systems has grown thanks to their assistance in improving the system stability, power efficiency, voltage profile, climate, and economic advantages. In specific, the DG is capable of:

1) Reducing greenhouse emissions to protect the atmosphere [1].

2) Giving easy solutions to catch the growth of load.

3) Stopping the rapid expansion of the transmission network which minimizes the transmission and distribution losses.

Furthermore, the load efficiency and power quality would increase if the DGs are properly regulated [2].

The idea of microgrid (MG) is shined up due to the rapid increase of the DG penetration in the power system. The MG contains multiple DGs and different loads. It can work either grid linked or in an autonomous operation mode [3]. In the first mode, the MG is linked to the grid. In addition, the power balance between the load and the microgrid generation is not needed because any shortfall in the power will be supplied from the grid. Also, any extra power will be drained by the grid. Meanwhile, in the second mode, the microgrid is separated from the grid. In addition, the DG has to preserve the equilibrium of generation – demand. Moreover, the DG regulates the voltage and frequency in this mode of operation to keep them within limits.

The advanced control methods are utilized in autonomous mode to ensure robust and safe operation. These methods can be classified into three major groups: (1) droop-based, (2) centralized control, and (3) multivariable and servomechanism (MVAS) techniques. In [4], the droop-based method is used to adjust the current of the DG units in a microgrid during the stand-alone mode. The benefits of using the droop-based control are its ability to independently

This article has been accepted for publication in a future issue of this journal, but has not been fully edited. Content may change prior to final publication. Citation information: DOI 10.1109/ACCESS.2021.3091496, IEEE Access

control distributed energy resource units (DERs) without contact between them. Its principal downside is, however, not being able to deal with nonlinear systems like load dynamics, which affect the system transient response [5]. In comparison, centralized control strategies require high bandwidth connections, and any loss of such connections can lead to a breakdown in the microgrid [6]. Finally, MVAS controllers are utilized in DG for autonomous mode [7]. Though, its inconvenience is the high complexity. Meanwhile, the PI controller is the best. It has always led among the others in the nonlinear system due to its high margin of stability. Owing to the responsive impact of such parameter, tuning the PI controller faces great difficulties. Therefore, many metaheuristic algorithms have been improved in order to overcome those difficulties, such as particle swarm optimization (PSO) [8], sunflower optimization algorithm (SFO) [9-10], hybrid GWO-PSO optimization technique [11], genetic algorithm (GA) [12], hybrid firefly and particle swarm optimization technique [13], Harris hawks optimization Method [14], marine predators algorithm [15], hierarchical model predictive control [16], Tabu search [17], quasi-oppositional selfish herd optimization (QSHO) [18], Cuttlefish optimization algorithm (CFA) [19], and teaching-learning based optimization [20]. Each of those techniques has its benefits and drawbacks [21].

B. Research gap and motivation

The optimization approaches have many limitations, such as dynamic systems, high storage demands, and high microprocessor capacities, etc. These drawbacks mean that new control procedures, including adaptation techniques, are needed. In [22], adaptive control based on an affine projection algorithm is presented. Faster integration and less machine complexity than optimization strategies were demonstrated. The previous adaptive technique also demonstrated certain attractive stuffs such as the coefficient vector. This technique monotonously approaches the real data regardless of the inputs, as stated in [23]. In [24], a new adaptive control based on set-membership engine algorithm is provided with improved performance than other techniques. The continuous p-norm mixed technique is presented as a new adaptive control of the VS, which rapidly updates the fuzzy inference system in [25]. In [26], the improved multiband-structured subband adaptive filter (IMSAF) algorithm-based self-tuned PI controller is employed to adjust the interface voltage source converters through a cascaded control structure. In [27], the improved zero attracting quaternion-valued least mean square (IZAQLMS) control approach with high DC offset rejection capability is used to improve the power quality of the grid current and to ensure the unity power factor operation of the grid.

The authors have proven the pioneer performance of the adaptive control algorithms over the conventional algorithms, SFO and PSO, in terms of less-computational complexity, better convergence, and lowest mean square error. Moreover, a class of reinforcement learning algorithms is not applicable for simple problem's solution as it requires huge data and lots of calculations.

This paper suggests a new adaptive technique titled as the least mean (LM) and square root of exponential (SRE) technique. The normalization of this technique is induced by the use of a negative absolute error exponent between [0, 1]. Furthermore, LMSRE has constants (μ and α) that combine rapid convergence and stability with minimal error.

C. Contribution and paper organization

The major contributions of this paper are:

1) Evaluation of the newly proposed LMSRE algorithm when applied to adapt PI controllers to enhance the MG system performance,
2) Testing the reliability of the proposed technique by exposing the system to several different environments, which are i) disconnect the system from the grid (islanding), ii) autonomous system exposure to load variability, and iii) autonomous system exposure to symmetrical faults,
3) Checking the validity of the presented adaptive control through matching its results with those obtained using the SFO and PSO algorithms.

The remaining sections of the paper are organized as follows: Section 2 presents the system modeling. Section 3 presents the control strategy. Section 4 presents the modeling stage using Response Surface Methodology (RSM), SFO and the suggested adaptive PI controller based on LMSRE technique. Section 5 presents the simulation results and discussion. Finally, the conclusion is presented in Section 6.

II. System Modelling

Fig.1 presents a single line diagram (SLD) of an MG, which consists of 3 DGs linked with each other by transmission lines. The DGs are linked to the PCC, which is linked to the grid by a transmission line (TL). Each DG consists of DC source linked to pulse width modulation (PWM) (2 levels). The PWM is linked to a Δ - Y transformer by a series filter to achieve a better quality of output power. A three-stage complex RLC load is attached to the transformer to reflect the local load. The MG data are stated in Table 1.

The system is working either in grid linked or in autonomous operation mode. In the grid linked mode, the DG unit runs in active and reactive power control mode. It is important to remember that the voltage and frequency are maintained by the grid. On the other hand, in the autonomous operation mode, the DG has to preserve the equilibrium of generation – demand. Also, it regulates the voltage and frequency to keep them within limits. This research focuses on enhancing the MG during the autonomous operation mode using the cascaded control scheme, which is discussed in the next section.

This article has been accepted for publication in a future issue of this journal, but has not been fully edited. Content may change prior to final publication. Citation information: DOI 10.1109/ACCESS.2021.3091496, IEEE Access

III. CONTROL STRATEGY

In this paper, the conventional cascaded control system is utilized in maintaining the voltage at the point of common coupling (PCC) for each DG. The reference voltages ($V_{conv\_a}^*$, $V_{conv\_b}^*$, $V_{conv\_c}^*$) are extracted by the transformation of the dq reference voltages ($V_{conv\_d}^*$, $V_{conv\_q}^*$) using the transformation angle (θ_{PLL}). $V_{conv_d}^*$and $V_{conv\_q}^*$ are extracted with the help of four PI controllers as shown in Fig. 2. θ_{PLL} is excluded from the phase-locked loop (PLL), which sets the grid voltages at its entry level. The firing pulses of the inverter switches are obtained from the comparator, which compares the reference voltages ($V_{conv\_a}^*$, $V_{conv\_b}^*$, $V_{conv\_c}^*$) with a triangular signal. V_d and V_q are the direct and the quadrature axis voltages extracted by the transformation from the stationary frame to the dq frame.

The four PI controllers' gains are extracted by the aid of the proposed adaptive technique and the other optimization techniques. It is more stated in details in the Section IV.

Table 1 System Data for MG

Transformer parameters
Δ/Y = 0.6/13.8 KV
Load data
Load 1: C_1 = 50 µF, R_{l1} = 9Ω, R_{l2} = 150 Ω, L_1 = 0.6 H.
Load 2:C_2 = 42 µF, R_{22} = 5 Ω, R_{l2} = 150 Ω, L_2 = 0.4 H.
Load 3:C_3 = 33 µF, R_{33} = 20 Ω, R_{l2} = 150 Ω, L_3 = 1.5 H.
Transmission Line data
TL1: R_{TL1}= 0.7 Ω, L_{TL1} = 0.5 mH.
TL2: R_{TL2} = 1.5 Ω, L_{TL2} = 0.9 mH.
Filter parameters
R_f = 1.5m Ω, X_f = 0.5m H
Grid data
V = 13.8 KV, R_g=0.2 Ω, L_g=0.3 mH

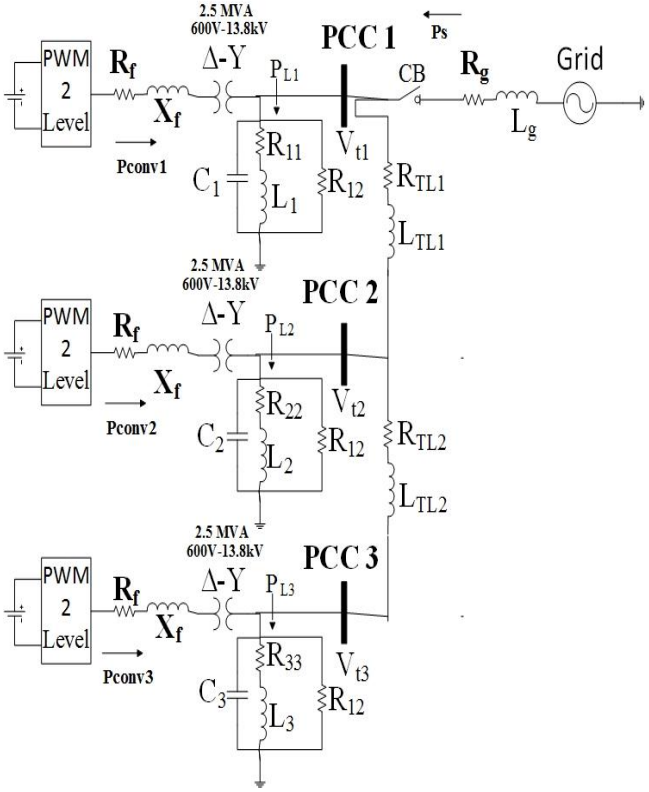

Fig.1. SLD of MG

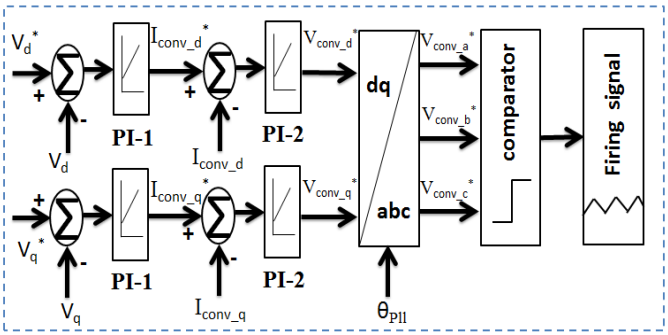

Fig. 2. Conventional control technique for autonomous operation mode.

IV. MODELING STAGE:

A. The RSM

Thanks to its performance in analysing many systems, the value of the RSM technique is quickly increasing. The RSM is a mathematical technique. It empirically develops models by extracting association between control and reaction parameters by means of a good statistical technique [28]. Through the data collected, the PSCAD program makes a great contribution to the simulation stage. The data extracted from the PSCAD is used as input of the RSM system for the different scenarios. For the introduced research, the RSM input data is decided to be the settling time (T_{set}), maximum percentage undershoots (MPUS), steady-state error (E_{ss}) and maximum percentage overshoots (MPOS) of the terminal voltage. The central composite design (CCD) scheme is utilized to run the 2nd order RSM model for more reliable

This article has been accepted for publication in a future issue of this journal, but has not been fully edited. Content may change prior to final publication. Citation information: DOI 10.1109/ACCESS.2021.3091496, IEEE Access

performance. The RSM is applied by the MINITAB software.

The minimization of the MPOS, MPUS, T_{set}, and E_{ss} for the three scenarios describe the multi-objective function. Eq. (1) is the objective function, which is extracted from the RSM model for scenario 1, which is used in the optimization process for both SFO and PSO.

$$X_i = Z_1 + Z_2k_1 + Z_3k_2 + Z_4k_3 + Z_5k_4 + Z_6k_1^2 + Z_7k_2^2 + Z_8k_3^2 + Z_9k_4^2 + Z_{10}k_1k_2 + Z_{11}k_1k_3 + Z_{12}k_1k_4 + Z_{13}k_2k_3 + Z_{14}k_2k_4 + Z_{15}k_3k_4 \quad (1)$$

where i=1, 2, 3, 4,
Z1, Z2…, Z15=the RSM model constants obtained for each scenario which are presented in [29].

B. The SFO Algorithm

The development of soft computing power is the major motivation to use SFO in optimizing many problems. The SFO is a heuristic technique that is motivated by nature. Its core idea is mainly simulating the orientation of the sunflowers to receive sunlight [9]. The sunflower motion is repeated every day, which starts in the morning following the sunlight. At the evening, the sunflower returns to the initial position waiting for the sunlight. Just one pollen gamete is presumed by each sunflower. Radiation from inverse square rule here is essential. Since the sunflowers take next to the sun a massive amount of heat from the sun compared to those farther ones that of the distant ones. The sunflowers are next to the sun lean towards quiet in this spot [9]. Eq. (2) shows the heat absorbed for each population.

$$Q_i = \frac{P}{4\pi r_i^2} \quad (2)$$

where P is known as the source of the power. r_i is the space between the recent best and population i.

Motions of sunflowers is described by Eq. (3) [10]:

$$\vec{s}_i = \frac{X^* - X_i}{||X^* - X_i||}, \quad i = 1,2,\dots,n_p. \quad (3)$$

Eq. (4) shows the sunflowers' step in the direction of "s":

$$d_i = T \times P_i(X_i + X_{i-1}) \times \left|\left|X_i + X_{i-1}\right|\right| \quad (4)$$

where T is a fixed value, which describes an "inertial" movement of the sunflowers, $P_i(||X_i + X_{i-1}||)$ is the pollination probability.
The restriction on these steps is stated in Eq. (5):

$$d_{max} = \frac{||X_{max} - X_{min}||}{2 \times N_{pop}}, \quad (5)$$

where X_{max} and X_{min} are defined as the upper and lower bounds. N_{pop} shows the total number of populations.

The next plant is given by this eq.:

$$\vec{X}_{i+1} = \vec{X}_i + d_i \times \vec{s}_i \quad (6)$$

The SFO steps are stated as:

1) Generation of random population.
2) The best population is assumed to be the new sun.
3) The other populations adjust their orientation towards the sun.

A flowchart for SFO, is shown in Fig. 3 for further explanations.

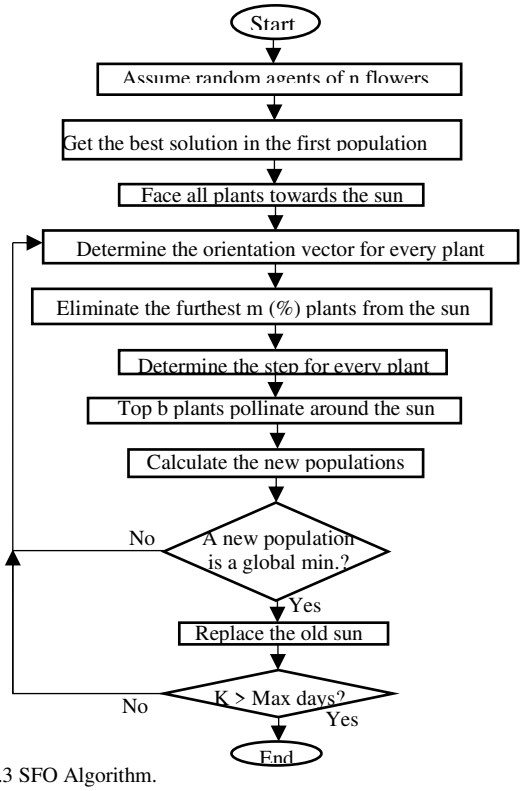

Fig.3 SFO Algorithm.

C. Optimization using SFO

The multi-objective function is stated in Eq. (1). It relies on the weighting method [30], and it is used in the SFO code which is presented in [31]. The settings of the SFO and the weights used in the multi objective function are stated in [29].

D. LMSRE algorithm

The adaptive filtering algorithms (AFA) are typically used to find the impulse response weight vector (W_0) filter [32] as presented in Fig. 4. The input C_k is applied to a Gaussian noise N_k passing through FIR filter. Therefore, it relies on the error e_k, which is presented in Eq. (7) [32].

$$e_k = d_k - W_k^T C_k \quad (7)$$

This article has been accepted for publication in a future issue of this journal, but has not been fully edited. Content may change prior to final publication. Citation information: DOI 10.1109/ACCESS.2021.3091496, IEEE Access

where k is the number of iterations, W_k defines the expected vector of the weight. d_k defines the forecasted signal as in Eq. (8)

$$d_k = W_0^T C_k + N_k \quad (8)$$

The iteration of the AFAs relies on the steepest descent algorithm as in Eq. (9).

$$W_{k+1} = W_k - \mu \nabla_W j(W_k) \quad (9)$$

where μ shows the step-size. ∇ is the grad. operative. J defines the cost function, as presented in Eq. (10).

$$j(W_k) = |e_k| + 2\sqrt{1 + \exp(-|e_k|)} - 2\sqrt{2} \quad (10)$$

Then, the gradient of the cost function is obtained as follows:

$$\nabla_W j(W_k) = \frac{\partial}{\partial W_k}|e_k| + 2\frac{\partial}{\partial W_k}\sqrt{1 + \exp(-|e_k|)} \quad (11)$$

$$\frac{\partial}{\partial W_k}|e_k| = \frac{\partial}{\partial W_k}|d_k - W_k^T C| = \text{sign}(e_k).(-C_k) \quad (12)$$

$$\frac{\partial}{\partial W_k}\sqrt{1 + \exp(-|e_k|)} = \frac{-\exp(-|e_k|)\frac{\partial}{\partial W_k}|e_k|}{2\sqrt{1 + \exp(-|e_k|)}} \quad (13)$$

Then, substitute Eq. (12) and Eq. (13) into Eq. (11) to get Eq. (14) and Eq. (15).

$$\nabla_W j(W_k) = \left[\text{sign}(e_k).(-C_k) - \frac{\exp(-|e_k|)\text{sign}(e_k).(-C_k)}{\sqrt{1 + \exp(-|e_k|)}}\right] \quad (14)$$

$$\nabla_W j(W_k) = \text{sign}(e_k).(-C_k) - \left[\frac{\exp(-|e_k|)}{\sqrt{1 + \exp(-|e_k|)}}\right] \quad (15)$$

Assume that

$$\beta_k = 1 - \frac{\exp(-|e_k|)}{\sqrt{1 + \exp(-|e_k|)}} \quad (16)$$

Then, substitute Eq. (15) into Eq. (9) to get Eq. (17).

$$W_{k+1} = W_k - \mu_k.\beta_k.\text{sign}(e_k).C_k \quad (17)$$

where μ_k is to differ with the variance of the error, for the huge error, μ_k should be large for rapid convergence. On the other hand, for a small error, μ_k must be minimized. So, β_k varies from [0, 1], which is minimized for tiny error and vice versa. So, μ_k varies proportionally to the β_k as below.

$$\mu_k = \mu.\beta_k^{\alpha-1} \quad (18)$$

where μ and α are responsible for variation of μ_k, then, substitute Eq. (18) into Eq. (17) to obtain eq. Eq. (19).

$$W_{k+1} = W_k - \mu.\beta_k^{\alpha}.\text{sign}(e_k).C_k \quad (19)$$

E. Optimization using LMSRE

The PI Controller Parameters are modified using the LMSRE algorithm Based on eq. (19). The updated PI parameters can be defined below:

$$k_{p(k+1)} = k_{p(k)} + \Delta k_{p(k)} \quad (20)$$

$$T_{i(k+1)} = T_{i(k)} + \Delta T_{i(k)} \quad (21)$$

$$\Delta k_{p(k)} = \Delta T_{i(k)} = \mu.\beta_k^{\alpha}.\text{sign}(e_k).C_k \quad (22)$$

The initial PI parameter values (k_p and T_i) for the 6 PI controllers (V_1 to V_6) are obtained with the trial-and-error method expressed in Table 2.

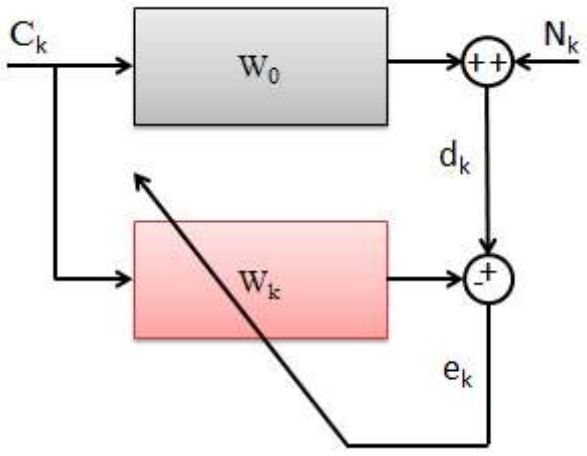

Fig. 4. System identification model of FIR filter

This article has been accepted for publication in a future issue of this journal, but has not been fully edited. Content may change prior to final publication. Citation information: DOI 10.1109/ACCESS.2021.3091496, IEEE Access

Table 2 The initial PI parameter values for scenario 1

controller	V_1	V_2	V_3	V_4	V_5	V_6
Initial k_p	5	3	5	3	5	3
Initial T_i	0.003	0.3	0.003	0.3	0.003	0.3

V. Comparative evaluation for the SFO, PSO and LMSRE results

This section's primary goal is to proof the validity and to display the effectiveness of the suggested control strategy to sustain the PCC voltage within the required limits in various MG operating conditions. The proposed practicality of the control plan is shown by the data of simulation which is extracted from PSCAD/EMTDC software. The results of SFO and PSO in [29] are compared with the obtained from LMSRE, the constants of the LMSRE are assumed to be (μ=0.01), and (α = 5.5). For more accuracy, 50 µs is selected for both time step and the channel plot time. The system is evaluated under several different environments which are: 1) Disconnection of the system from the grid (islanding), 2) Autonomous system exposure to load variability, and 3) Autonomous system exposure to a symmetrical fault. More detailed discussion is presented in the next sections.

A. Scenario 1 (autonomous operation)

In this Scenario, the MG is in a steady-state condition in the grid-connected mode. The MG is suddenly disconnected from the utility grid (autonomous mode) at t=2 s. The optimal PI parameters values in each DG for LMSRE, SFO and PSO are listed in Table 3. Figs. 5 (a, b, c) present the PCC voltage profile in each DG for LMSRE, SFO and PSO. Figs. 6 (a, b, c) present the Real and imaginary powers for the load in each DG for LMSRE, SFO and PSO. It is valuable to mention that, in Fig. 5a, the MPUS for autonomous mode responses of the PCC1 voltage for the proposed technique are less than 8%. Moreover, the settling time based on 2% criterion is 5 ms and the Ess is 0.32%. Therefore, the proposed control technique shows minimum overshoots, rapid damping and perfect Ess. The voltage undershoot of the DG 3 is slightly lower than other DGs owing to its higher distance from the fault place, as seen in Fig. 5c. It is valuable to mention that the LMSRE is pioneer in MPUS, MPOS, test, and is compared to SFO and PSO. This proofs the flexibility, justification, and applicability of the introduced adaptive technique (LMSRE) over SFO and PSO.

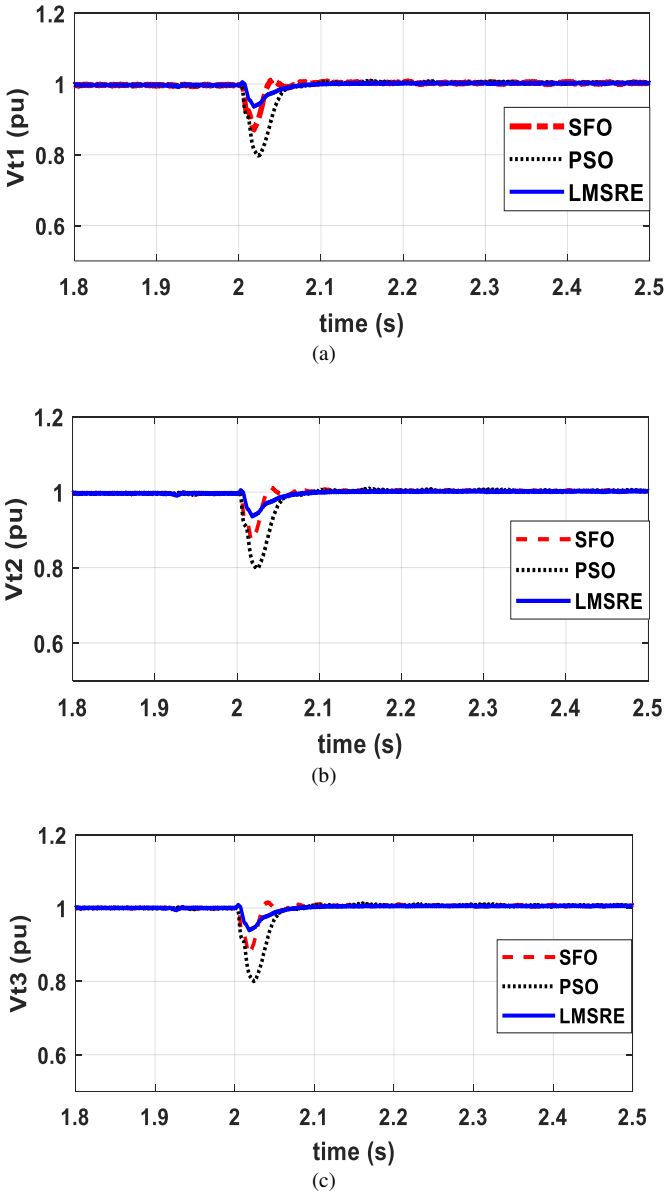

Fig.5. Output results for LMSRE, SFO and PSO of Scenario 1. (a) Voltage profile of DG 1. (b) Voltage profile of DG 2. (c) Voltage profile of DG 3.

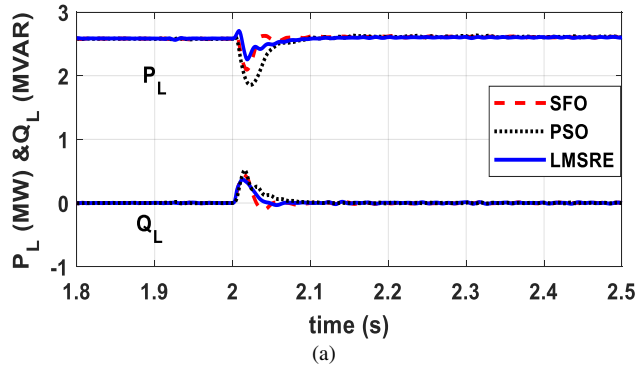

This article has been accepted for publication in a future issue of this journal, but has not been fully edited. Content may change prior to final publication. Citation information: DOI 10.1109/ACCESS.2021.3091496, IEEE Access

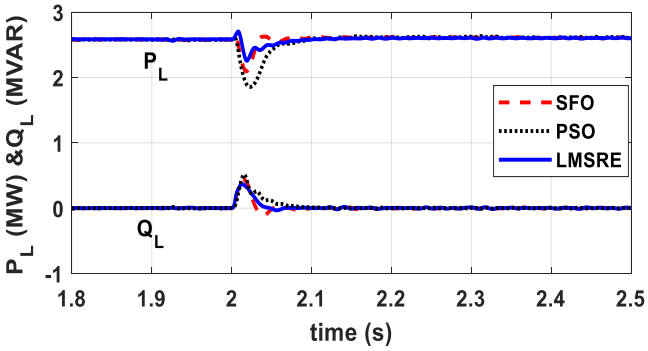

(b)

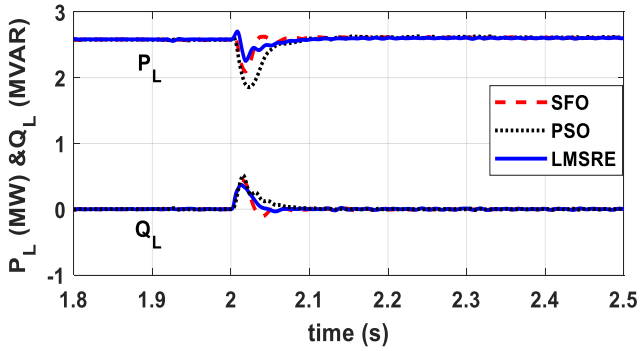

(c)

Fig.6. Output results for LMSRE, SFO and PSO of Scenario 1. (a) Real and reactive powers for the load in DG 1. (b) Real and imaginary powers for the load in DG 2. (c) Real and imaginary powers for the load in DG 3.

Table 3 the Results of LMSRE, SFO and PSO for Scenario1 in the 3 DGs

Point Of comparison	LMSRE	SFO	PSO
Scenario 1 DG 1			
MPUS	7.9%	12.905%	20.26%
Tset	0.0461 s	0.033 s	0.054 s
Ess	0.32%	0.35%	0.4%
Scenario 1 DG 2			
MPUS	7.898%	12.86%	20.1%
Tset	0.0461 s	0.0326 s	0.0535 s
Ess	0.3%	0.36%	0.405%
Scenario 1 DG 3			
MPUS	7.57%	12.6%	19.975%
Tset	0.0432 s	0.0322 s	0.0531 s
Ess	0.31%	0.32%	0.402%

B. Scenario 2 (load changing)

In this Scenario, the MG is run in the islanded mode. The MG originally runs with the RLC loads, which is mentioned in Table 1. R12 is changed from 150 Ω to 300 Ω at t=3 s and is returned to its initial state at t=3.4 s. The optimal PI parameters values in each DG for LMSRE, SFO and PSO are listed in Table 4. Figs. 7 (a, b, c) present the PCC voltage profile in each DG for LMSRE, SFO and PSO. Figs. 8 (a, b, c) present the Real and imaginary powers for the load in each DG for LMSRE, SFO and PSO. It is valuable to mention that, in Fig. 7a, the MPUS and MPOS for the load changing responses of the PCC1 voltage for the proposed technique are less than 3%. Moreover, the settling time based on 2% criterion is 40 ms and the E_{ss} is 0.43%. Therefore, the proposed control technique shows minimum overshoots, rapid damping and perfect E_{ss}. The voltage overshoots of the DG 3 are slightly lower than other DGs owing to its higher distance from the disturbance place, as seen in Fig. 7c. It is valuable to realize that, in Fig. 8a, the active power of DG 1 load decreased from 2.6 MW to 0.5 MW and back to its initial state smoothly at t=3.4 s. On the other hand, the active powers for the other DG loads have rapid damping with smaller fluctuations. It is valuable to mention that the LMSRE pioneer in MPUS, MPOS, T_{set}, and E_{ss} compared to SFO and PSO, which proof the flexibility, justification, and applicability of the introduced adaptive technique (LMSRE) over SFO and PSO.

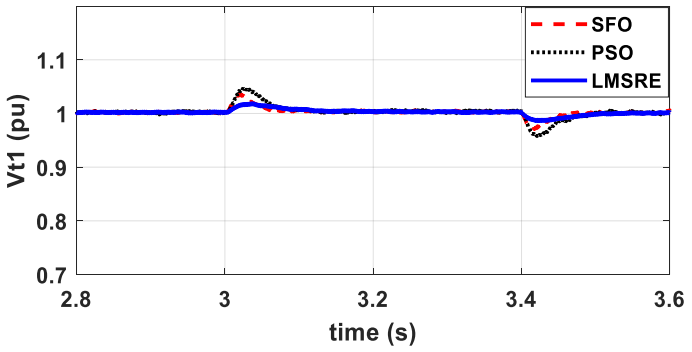

(a)

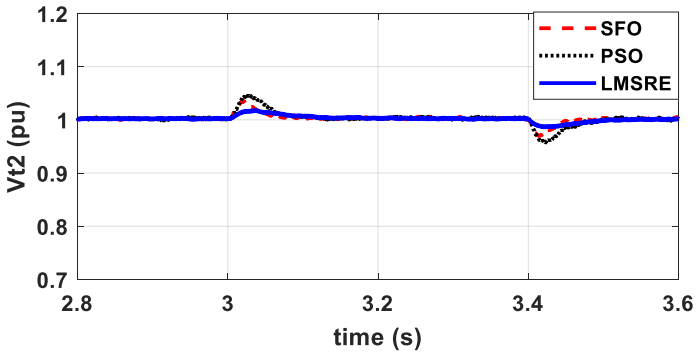

(b)

This article has been accepted for publication in a future issue of this journal, but has not been fully edited. Content may change prior to final publication. Citation information: DOI 10.1109/ACCESS.2021.3091496, IEEE Access

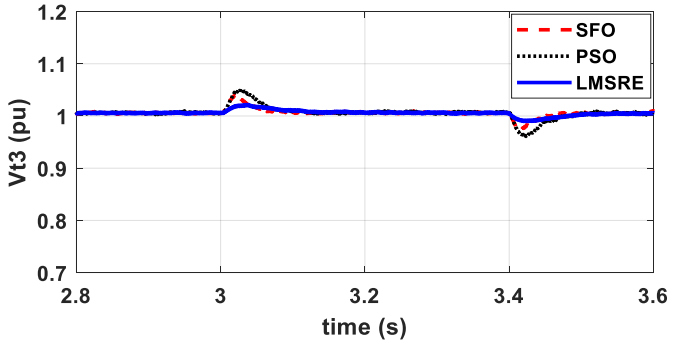

(c)

Fig.7. Output results for LMSRE, SFO and PSO of Scenario 2. (a) Voltage profile of DG 1. (b) Voltage profile of DG 2. (c) Voltage profile of DG 3.

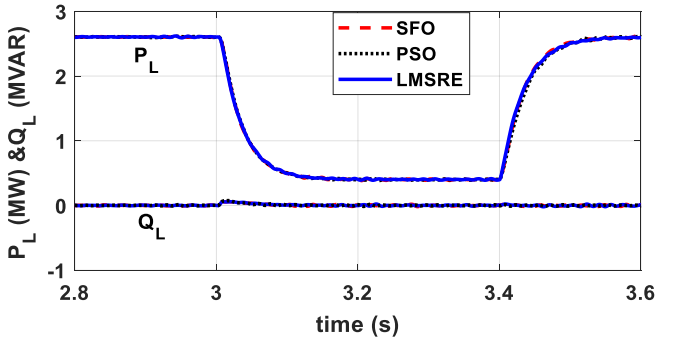

(a)

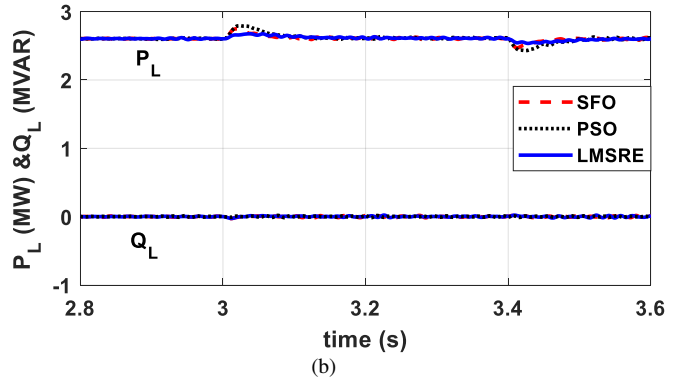

(b)

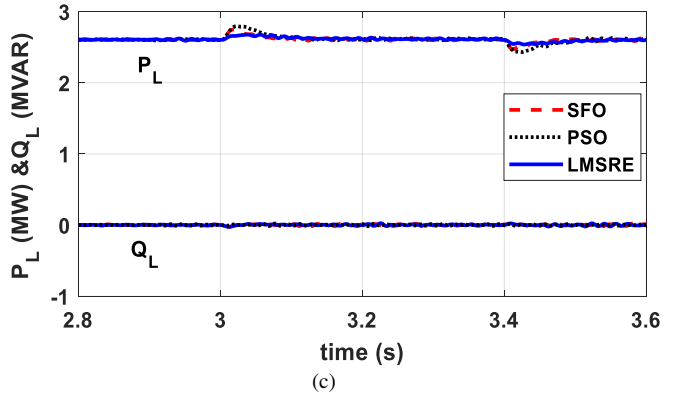

(c)

Fig.8. Output results for LMSRE, SFO and PSO of Scenario 2. (a) Real and imaginary powers for the load in DG 1. (b) Real and imaginary powers for the load in DG 2. (c) Real and imaginary powers for the load in DG 3.

Table 4 the Results of LMSRE, SFO and PSO for Scenario2 in the 3 DGs

Point Of comparison	LMSRE	SFO	PSO
Scenario 2 DG 1			
MPUS	1.88%	3.2%	4.3%
MPOS	2.22%	3.97%	5%
Tset	0.401 s	0.43 s	0.45 s
Ess	0.43%	0.44%	0.48%
Scenario 2 DG 2			
MPUS	1.882%	3.12%	4.275%
MPOS	2.1%	3.61%	4.64%
Tset	0.403 s	0.4289 s	0.445 s
Ess	0.52%	0.665%	0.69%
Scenario 2 DG 3			
MPUS	1.5%	2.745%	3.909%
MPOS	2.53%	3.6%	4.7%
Tset	0.4015 s	0.424 s	0.443 s
Ess	0.737%	1.032%	1.07%

C. Scenario 3 (symmetrical fault)

In this Scenario, the MG is at steady-state in an islanded mode. Then, a symmetrical fault is suddenly occurs at PCC 1 at t=4 s and back to a healthy state at t= 4.1 s. The optimal PI parameters values in each DG for LMSRE, SFO and PSO are listed in Table 5. Figs. 9 (a, b, c) present the PCC voltage profile in each DG for LMSRE, SFO and PSO. Figs. 10 (a, b, c) present the real and imaginary powers for the load in each DG for LMSRE, SFO and PSO. It is valuable to mention that, in Fig. 9a, the T_{set} based on 2% criterion for the fault responses of the PCC1 Voltage for the proposed technique is 49 ms and the Ess is 0.25%. Therefore, the proposed control technique shows rapid damping and perfect Ess. The voltage overshoots of the DG 3 are slightly lower than other DGs owing to its higher distance from the fault place, as seen in Fig. 9c. It is valuable to mention that the LMSRE has slightly higher overshoots. On the other hand, it shows very fast damping and perfect Ess compared to SFO and PSO. This proofs the flexibility, justification, and applicability of the introduced adaptive technique (LMSRE) over SFO and PSO.

This article has been accepted for publication in a future issue of this journal, but has not been fully edited. Content may change prior to final publication. Citation information: DOI 10.1109/ACCESS.2021.3091496, IEEE Access

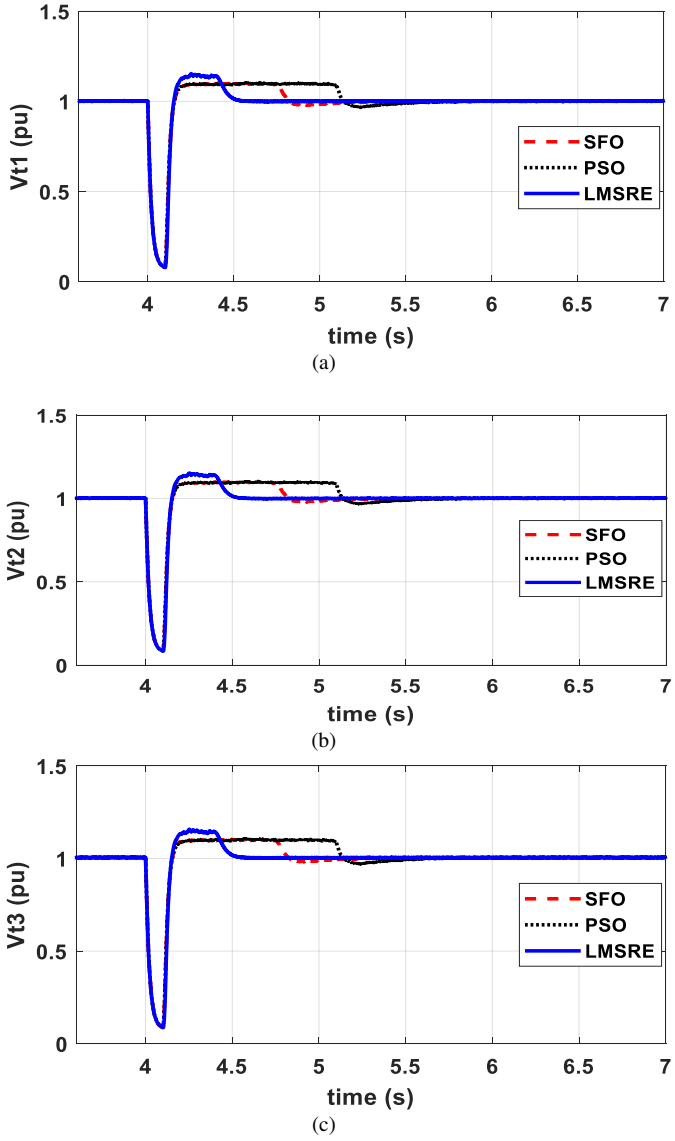

Fig.9. Output results for LMSRE, SFO and PSO of Scenario 3. (a) Voltage profile of DG 1. (b) Voltage profile of DG 2. (c) Voltage profile of DG 3.

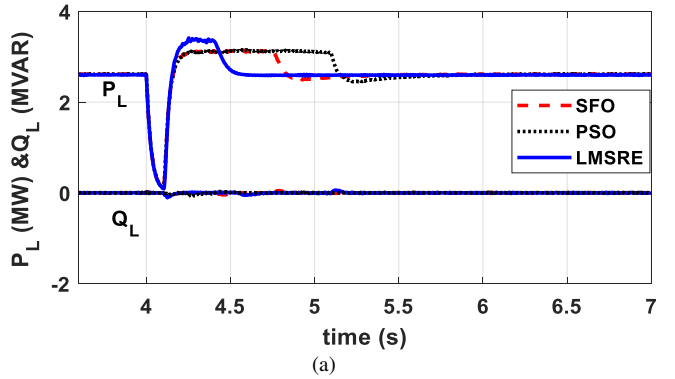

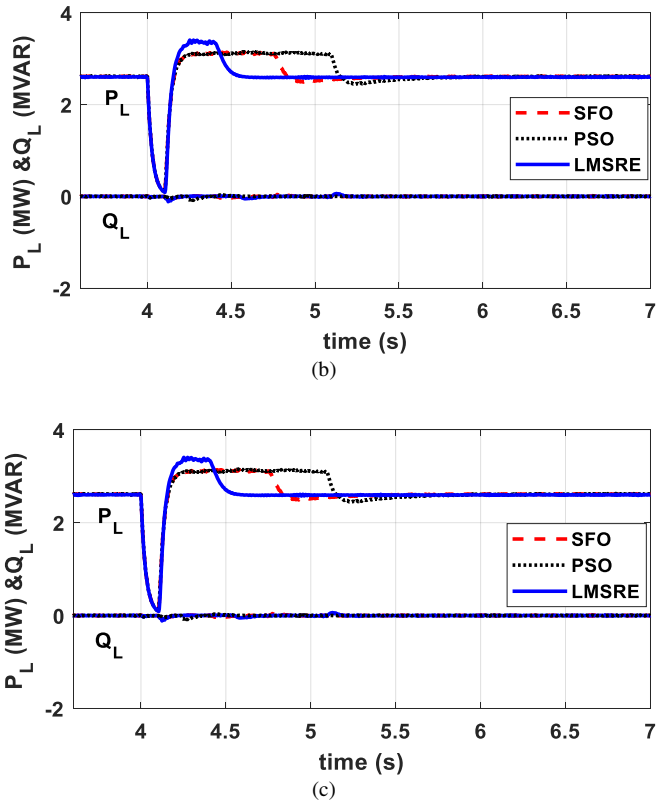

Fig.10. Output results for LMSRE, SFO and PSO of Scenario 3. (a) Real and imaginary powers for the load in DG 1. (b) Real and imaginary powers for the load in DG 2. (c) Real and imaginary powers for the load in DG 3.

Table 5 the Results of LMSRE, SFO and PSO for Scenario3 in the 3 DGs

Point Of comparison	LMSRE	SFO	PSO
Scenario 3 DG 1			
MPUS	92.16%	91.638%	93.108%
MPOS	15.4%	10.705%	10.956%
Tset	0.4915 s	0.9654 s	1.3901 s
Ess	0. 25%	0.46%	0.55%
Scenario 3 DG 2			
MPUS	91.67%	92.135%	92.14%
MPOS	15.402%	10.3505%	10.604%
Tset	0.4916 s	0.9654 s	1.3901 s
Ess	0.337%	0.495%	0.63%
Scenario 3 DG 3			
MPUS	91.312%	93.106%	91.64%
MPOS	15.824%	10.205%	10.59%
Tset	0.4972 s	0.8069 s	1.384 s
Ess	0.67%	0.842%	1.02%

Vi. Conclusions

This paper has introduced a new implementation of adaptive PI controller optimum design scheme of multiple PI controllers' parameters to boost microgrid efficiency. Six PI controllers are utilized in the control scheme. The results showed that the presented controller is able to

simultaneously retain the real and imaginary power. It also regulates the reference voltages. The results show a quick damping in transient response with a rapid T_{set} and a small E_{ss} under a different microgrid operating condition. The system is evaluated under several different environments which are: 1) disconnect the system from the grid (islanding), 2) autonomous system exposure to load variability, and 3) autonomous system exposure to a symmetrical fault. The proposed practicality of the control plan is shown by the data of the simulation which is extracted from PSCAD/EMTDC software. The strength of the suggested adaptive control is confirmed through matching its results with that obtained using the SFO and the PSO techniques. LMSRE-based adaptive PI controller has achieved lower values of the transient responses in the autonomous operation of the MG over that obtained using the SFO and the PSO. In scenario 1, The MPUS of the voltage profile using the suggested adaptive control is decreased by 38.7% and 61% over that using the SFO and the PSO, respectively. In scenario 2, The MPUS of the voltage profile using the suggested adaptive control is decreased by 41% and 56% over that using the SFO and the PSO, respectively. Moreover, the MPOS of the voltage profile using the LMSRE is decreased by 44% and 55.6% over that by using the SFO and the PSO, respectively. In scenario 3, The T_{set} of the voltage profile using the suggested adaptive control is decreased by 49% and 64% over that using the SFO and the PSO. Furthermore, the E_{ss} of the voltage profile using the LMSRE is decreased by 45.6% and 54.5% over that using the SFO and the PSO, respectively. The future work will focus on intensifying the proposed LMSRE-based adaptive PI controller to adjust the power system applications, energy storage devices, and smart grids, achieving optimum responses in the renewable energy conversion system.

VII. REFERENCES

[1] Hasanien, H.M., Matar, M.: 'A fuzzy logic controller for autonomous operation of a voltage source converter-based distributed generation system', *IEEE Trans. Smart Grid*, 2015, 6, (1), pp. 158–165.

[2] N. Hatziargyriou, H. Asano, R. Iravani, and C. Marnay, "Microgrids," IEEE Power Energy Mag., vol. 5, no. 4, pp. 78–94, Jul./Aug. 2007.

[3] Sasan, G., Mohammad, A., Saha, S.: 'Control strategy for dispatchable distributed energy resources in islanded microgrids', IEEE Trans. Power Syst., 2018, 33, (1), pp. 141–152

[4] Matayoshi, Hidehito, et al. "Islanding operation scheme for DC microgrid utilizing pseudo Droop control of photovoltaic system." Energy for Sustainable Development 55 (2020): 95-104.

[5] De Brabandere, K., Bolsens, B., Van den Keybus, J., et al.: 'A voltage and frequency droop control method for parallel inverters', IEEE Trans. Power Electron., 2007, 22, (4), pp. 1107–1115

[6] Guerrero, J.M., Hang, L., Uceda, J.: 'Control of distributed uninterruptible power supply systems', IEEE Trans. Ind. Electron., 2008, 55, (8), pp. 2845– 2859

[7] Roszak, Bartek, and Edward J. Davison. "The Multivariable Servomechanism Problem for Positive LTI Systems $$." IEEE transactions on automatic control 55.9 (2010): 2204-2209.

[8] Hinojosa, V. H., and Araya, R., "Modeling a mixed-integer binary small-population evolutionary particle swarm algorithm for solving the optimal power flow problem in electric power systems," *Appl. Soft Comput*., vol. 13, no. 9, pp. 3839–3852, 2013.

[9] Shaheen, Mohamed AM, et al. "Optimal power flow of power systems including distributed generation units using sunflower optimization algorithm." IEEE Access 7 (2019): 109289-109300.

[10] Gomes, Guilherme Ferreira, Sebastiao Simões da Cunha, and Antonio Carlos Ancelotti. "A sunflower optimization (SFO) algorithm applied to damage identification on laminated composite plates." Engineering with Computers 35.2 (2019): 619-626.

[11] Shaheen, Mohamed AM, Hany M. Hasanien, and Abdulaziz Alkuhayli. "A novel hybrid GWO-PSO optimization technique for optimal reactive power dispatch problem solution." Ain Shams Engineering Journal (2020).

[12] Attia, A., Al-Turki, Y. A., Abusorrah, A. M., "Optimal power flow using adapted genetic algorithm with adjusting population size," *Electr. Power Compo. Syst*., vol. 40, no. 11, pp. 1285–1299, 2012.

[13] Abdullah, Nor Azliana, et al. "Forecasting Solar Power Using Hybrid Firefly and Particle Swarm Optimization (HFPSO) for Optimizing the Parameters in a Wavelet Transform-Adaptive Neuro Fuzzy Inference System (WT-ANFIS)." Applied Sciences 9.16 (2019): 3214.

[14] Shaheen, Mohamed AM, et al. "Optimal Power Flow of Power Networks with Penetration of Renewable Energy Sources By Harris hawks Optimization Method." 2020 2nd International Conference on Smart Power & Internet Energy Systems (SPIES). IEEE, 2020.

[15] Shaheen, Mohamed AM, et al. "A Novel Application of Improved Marine Predators Algorithm and Particle Swarm Optimization for Solving the ORPD Problem." Energies 13.21 (2020): 5679.

[16] Taher, Ahmed M., Hany M. Hasanien, Ahmed R. Ginidi, and Adel TM Taha. "Hierarchical Model Predictive Control for Performance Enhancement of Autonomous Microgrids." Ain Shams Engineering Journal (2021).

[17] Karamichailidou, Despina, Vasiliki Kaloutsa, and Alex Alexandridis. "Wind turbine power curve modeling using radial basis function neural networks and tabu search." Renewable Energy 163 (2021): 2137-2152.

[18] Barik, Amar K., and Dulal C. Das. "Coordinated regulation of voltage and load frequency in demand response supported biorenewable cogeneration-based isolated hybrid microgrid with quasi-oppositional selfish herd optimisation." International Transactions on Electrical Energy Systems 30.1 (2020): e12176

[19] Hussien, A. M., S. F. Mekhamer, and Hany M. Hasanien. "Cuttlefish Optimization Algorithm based Optimal PI Controller for Performance Enhancement of an Autonomous Operation of a DG System." 2020 2nd International Conference on Smart Power & Internet Energy Systems (SPIES). IEEE, 2020

[20] S. S. Reddy, P. R. Bijwe, "Efficiency improvements in meta-heuristic algorithms to solve the optimal power flow problem," *Electr. Power Energy Syst*., vol. 82, pp. 288-302, 2016.

[21] A. E. Chaib, H. R. E-H. Bouchekara, R. Mehasni, M. A. Abido, "Optimal power flow with emission and non-smooth cost functions using backtracking search optimization algorithm," *Int. J. Electr. Power Energy Syst*., vol. 81, pp. 64-77, 2016.

[22] Wang, Xiaoding, and Jun Han. "Affine Projection Algorithm Based on Least Mean Fourth Algorithm for System Identification." IEEE Access 8 (2020): 11930-11938.

[23] Lim, Jae Sung. "New adaptive filtering algorithms based on an orthogonal projection of gradient vectors." IEEE Signal Processing Letters 7.11 (2000): 314-316.

[24] S. Werner; P.S.R. Diniz, "Set-membership affine projection algorithm", IEEE Signal Processing Letters, Vol. 8, Issue: 8, Aug. 2001, Page(s): 231 – 235.

[25] S.M. Muyeen and Hany M. Hasanien, " Operation and control of HVDC stations using continuous mixed p-norm-based adaptive fuzzy technique", IET Generation, Transmission & Distribution, Vol. 11, Issue 9, 22 June 2017, p. 2275 – 2282.

[26] Soliman, M. A., Hasanien, H. M., Al-Durra, A., & Alsaidan, I. (2020). A Novel Adaptive Control Method for Performance Enhancement of Grid-Connected Variable-Speed Wind Generators. IEEE Access, 8, 82617-82629.

[27] Gupta, S., Verma, A., Singh, B., Garg, R., & Singh, A. (2020). IZAQ-LMS-based control of PV-battery interfaced microgrid in grid-connected and autonomous modes. IET Power Electronics, 13(17), 3999-4007.

[28] H. M. Hasanien, A. S. Abd-Rabou, and S. M. Sakr, "Design optimization of transverse flux linear motor for weight reduction and performance improvement using response surface methodology and genetic algorithms," IEEE Trans. Energy Convers., vol. 25, no. 3, pp. 598–605, Sep. 2010.

[29] Hussien, A. M., S. F. Mekhamer, and Hany M. Hasanien. " Sunflower Optimization Algorithm-Based optimal PI control for Enhancing the Performance of an Autonomous Operation of a Microgrid." Accepted in Ain Shams Engineering Journal (2020).

[30] I. Y. KimO. L. de WeckEmail, "Adaptive weighted sum method for multiobjective optimization: a new method for Pareto front generation", Structural and Multidisciplinary Optimization, Feb. 2006, Vol. 31, Issue 2, pp 105–116

[31] Mohamed Abdel-Basset, Laila A. Shawky, "Flower pollination algorithm: a comprehensive review", Artificial Intelligence Review, Springer Link, pp 1–25, March 2018.

[32] Qais, Mohammed H., Hany M. Hasanien, and Saad Alghuwainem. "A novel LMSRE-based adaptive PI control scheme for grid-integrated PMSG-based variable-speed wind turbine." International Journal of Electrical Power & Energy Systems 125: 106505.

A. M. Hussien received his B.Sc. degree in Electrical Engineering from Future University In Egypt, Faculty of Engineering, Cairo, Egypt, in 2014. From 2014, he is M.Sc student at Ain Shams University, Faculty of Engineering, Cairo, Egypt. Currently, he is TA at Future University in Egypt, Faculty of Engineering, Cairo, Egypt. His research interests include power systems operation, Microgrid, renewable energy systems.

Rania A. Turky received her B.Sc. and M.Sc. degrees in Electrical Power Engineering from Ain Shams University, Faculty of Engineering, Cairo, Egypt, in 2004 and 2010, respectively. She is now pursuing PhD degree at Ain Shams University. Her research interests include modern control techniques, power systems dynamics and control, energy storage systems, renewable energy systems, and smart grid.

Hany M. Hasanien (M 09, SM 11) received his B.Sc., M.Sc. and Ph.D. degrees in Electrical Engineering from Ain Shams University, Faculty of Engineering, Cairo, Egypt, in 1999, 2004, and 2007, respectively. From 2008 to 2011, he was a Joint Researcher with Kitami Institute of Technology, Kitami, Japan. From 2012 to 2015, he was Associate Professor at College of Engineering, King Saud University, Riyadh, Saudi Arabia. Currently, he is Professor at the Electrical Power and Machines Department, Faculty of Engineering, Ain Shams University. His research interests include modern control techniques, power systems dynamics and control, energy storage systems, renewable energy systems, and smart grid. Prof. Hasanien is an Editorial Board Member of *Electric Power Components and Systems Journal*. He is Subject Editor of IET Renewable Power Generation, Ain Shams Engineering Journal and Electronics MDPI. He has authored, co-authored, and edited three books in the field of electric machines and renewable energy. He has published more than 150 papers in international journals and conferences. His biography has been included in *Marquis Who's Who in the world* for its 28 edition, 2011. He was awarded Encouraging Egypt Award for Engineering Sciences in 2012. He was awarded Institutions Egypt Award for Invention and Innovation of Renewable Energy Systems Development in 2014. He was awarded the Superiority Egypt Award for Engineering Sciences in 2019. Currently, he is IEEE PES Egypt Chapter Chair and Editor in Chief of Ain Shams Engineering Journal.

Ahmed Al-Durra (S'07-M'10-SM'14) received his PhD in ECE from Ohio State University in 2010. He is a Professor in the EECS Department at Khalifa University, UAE. His research interests are applications of control and estimation theory on power systems stability, micro and smart grids, renewable energy systems and integration, and process control. He has one US patent, one edited book, 12 book chapters, and over 210 scientific articles in top-tier journals and refereed international conference proceedings. He has supervised/co-supervised over 25 PhD/Master students. He is leading the Energy Systems Control & Optimization Lab under the Advanced Power & Energy Center, an Editor for IEEE Transactions on Sustainable Energy and IEEE Power Engineering Letters, and Associate Editor for IEEE Transactions on Industry Applications, IET Renewable Power Generation, and Frontiers in Energy Research.